HOKKAIDO UNIVERSITY

Title	Vitamin K2 Attenuates Mitochondrial Damage in Renal Proximal Tubular Cells
Author(s)	Ho, Hsinjung; Aoki, Natsumi; Eguchi, Miki et al.
Citation	Journal of Agricultural and Food Chemistry, 73(35), 21857-21868 https://doi.org/10.1021/acs.jafc.5c01320
Issue Date	2025-05-21
Doc URL	https://hdl.handle.net/2115/97864
Rights	This document is the Accepted Manuscript version of a Published Work that appeared in final form in Journal of Agricultural and Food Chemistry, copyright © American Chemical Society after peer review and technical editing by the publisher. To access the final edited and published work see https://pubs.acs.org/articlesonrequest/AOR-MBUMPAWVSZUHEDRSTXBC.
Type	journal article
File Information	20250515 Vitamin K2 attenuates mitochondrial damage in renal proximal tubular cells_revised_V3_clean_copy.pdf



Hokkaido University Collection of Scholarly and Academic Papers : HUSCAP

Vitamin K2 attenuates mitochondrial damage in renal proximal tubular cells

Hsinjung Ho †, Natsumi Aoki †, Miki Eguchi †, Mingchen Gao †, Hirotaka Suzuki †, Mao Mikami †, Hitoshi Chiba †,‡, Shu-Ping Hui †,*

†Faculty of Health Sciences, Hokkaido University, Kita 12, Nishi 5, Kita-ku, Sapporo, Sapporo 060-0812, Japan.

‡Department of Nutrition, Sapporo University of Health Sciences, Nakanuma Nishi-4-2-1-15, Higashi-ku, Sapporo 007-0894, Japan.

Abstract

Excessive reactive oxygen species (ROS) levels cause oxidative stress, which leads to various diseases. Renal failure is associated with oxidative stress and mitochondrial dysfunction. Vitamin K1 (phylloquinone) and K2 (menaquinone) are essential for blood coagulation and bone formation. Vitamin K has been shown to have anti-inflammation, glucose metabolism regulation, and antiferroptosis functions. We investigated the impact of menaquinone-4 (MK-4) on oxidative stress and mitochondrial dysfunction in human renal proximal tubular cells. MK-4 protected cells from oxidative damage induced by L-buthionine-(S,R)-sulfoximine (BSO), a selective inhibitor of glutathione metabolism, by inhibiting cell death, mitochondrial ROS production, and lipid peroxidation. MK-4 also

reduced lactate production, prevented mitochondrial fragmentation, and improved mitochondrial respiratory function, indicating cytoprotective effects. Moreover, it enhanced intracellular ATP production and respiratory capacity even in the absence of oxidative stress. Thus, MK-4 plays an important role in mitochondrial function in renal proximal tubular cells.

Keywords: MK-4, oxidative stress, mitochondrial oxidative phosphorylation, ATP, mitophagy, renal function

1. Introduction

Reactive oxygen species (ROS) are essential for maintaining cellular homeostasis; however, excessive ROS production is implicated in a range of pathologies, including neurodegenerative diseases, cardiovascular disorders, and chronic kidney disease, all of which are linked to oxidative stress and mitochondrial dysfunction [1]. Mitochondria, a major source of ROS during ATP generation, can exacerbate oxidative stress when ROS levels are unregulated, leading to cellular damage and apoptosis. Renal proximal tubules are highly susceptible to mitochondria-related oxidative stress because of their high mitochondrial content and energy demands for nutrient reabsorption [2]. Accordingly, renal proximal tubules are considered critical targets in the study of kidney dysfunction.

Vitamin K (VK) is a micronutrient known primarily for its roles in blood coagulation and bone metabolism. It exists in two naturally occurring forms: vitamin K1 (phylloquinone) and vitamin K2 (menaquinone). One homolog of menaquinone, menaquinone-4 (MK-4) is the major form in animal tissues and converts from a part of ingested phylloquinone and menaquinones [3]. Recent studies have highlighted the novel antioxidant properties of VK, particularly within the mitochondria [4-5]. Despite increasing

43 evidence for the role of VK in mitigating oxidative stress, little is known about its
44 potential protective effects on mitochondria in renal proximal tubules. Given the
45 established association between mitochondrial dysfunction and renal impairment, this
46 study aimed to explore the cytoprotective effects of VK on proximal renal tubular cells
47 under oxidative stress.
48

49 2. Materials and methods

50 *2.1 Materials*

51 L-buthionine-(S, R)-sulfoximine (BSO) and menaquinone-4 (MK-4) were purchased
52 from Sigma-Aldrich (St. Louis, MO, USA). Dihydrorhodamine 123 (DHR123) and
53 warfarin were purchased from FUJIFILM Wako Pure Chemical Co. Ltd. (Tokyo, Japan).
54 ML162 was purchased from Cayman Chemical (Ann Arbor, MI, USA). iFSP1 was
55 purchased from Selleck Chemicals (Houston, TX, USA).

56 *2.2 Cell line and culture conditions*

57 HK-2 cells (American Type Culture Collection, Manassas, VA, USA), a human renal
58 proximal tubular cell line was cultured in Dulbecco's modified Eagle's medium (DMEM;

59 Nacalai Tesque, Kyoto, Japan), containing 1.0 g/L glucose, 10% fetal bovine serum (FBS;
60 Biosera, East Sussex, UK), and 1% penicillin-streptomycin solution (Nacalai Tesque), at
61 37°C in a humid atmosphere of 95% air and 5% CO_2. The medium was refreshed every
62 48 to 72 h until the desired confluency. All experiments were performed when the cells
63 reached 80% confluence.

64 *2.3 Cell viability and cytotoxicity*

65 HK-2 cells were cultured in 96-well plates, followed by the addition of BSO and MK-
66 4 for 48 h. The Cell Counting Kit 8 assay (Dojindo, Kumamoto, Japan) and the
67 Cytotoxicity LDH Assay-WST (Dojindo) were preformed to assess viability and toxicity
68 of the cells, respectively. The measurements were performed using a Wallac 1420 ARVO
69 Mx plate reader (PerkinElmer, Milford, MA, USA).

70 *2.4 mRNA expression levels*

71 HK-2 cells were cultured in six-well plates, followed by the addition of BSO and MK-
72 4 for 36 h. Total RNA was isolated using the NucleoSpin kit (TaKaRa Bio Inc., Shiga,
73 Japan) and the RNA was reverse transcribed into cDNA using a ReverTra Ace® qPCR
74 RT Master Mix with gDNA remover (TOYOBO, Osaka, Japan). Quantitative reverse

transcription polymerase chain reaction (qRT-PCR) was performed with THUNDERBIRD® SYBR® qPCR Mix (TOYOBO). The specificity and effectivity of PCR reactions were verified by melting curve analysis. qRT-PCR was conducted using a CFX Connect Real-Time PCR Detection System (Bio-Rad, Hercules, CA, USA), and β-actin was conducted as the reference gene to normalize the results using the $2^{-\Delta\Delta Ct}$ formula. Specific primer sequences used for PCR are listed in Table 1.

2.5 Malondialdehyde (MDA) levels

The thiobarbituric-acid-reactive substance (TBARS) assay is widely used to measure lipid oxidation [6]. A TBARS assay kit (Cayman Chemical) was used to determine the MDA levels in HK-2 cells. The cells were cultured in six-well plates, followed by the addition of BSO and MK-4 for 36 h. After washing with D-PBS(-) twice and collecting the samples, an SDS solution and the color reagent were added at a ratio of 1:1:4 (v/v/v) and the mixtures were heated at 100°C for 1 h. The samples were cooled and then centrifuged at 12,000 rpm for 10 min. Fluorescence (excitation/emission: 530/550 nm) was measured using an FP-6500 fluorescence spectrometer (Jasco Inc., Tokyo, Japan).

90 The MDA levels were normalized to the total protein concentration using a BCA protein
91 assay kit (Thermo Fisher Scientific, Waltham, MA).

92 *2.6 Glutathione (GSH)/oxidized GSH (GSSG) levels*

93 HK-2 cells were cultured in six-well plates, followed by the addition of BSO and MK-
94 4 for 3 h and 24 h. After washing with D-PBS(-) twice, cells were collected by
95 centrifugation at 200 × g, 4°C for 10 min. Collected cells were lysed in 80 μL of 10
96 mmol/L HCL, and 20 μL of 5% 5-sulfosalicylic acid solution was added. The GSH and
97 GSSG levels were measured using a GSSG/GSH quantification kit (Dojindo) following
98 to the manufacturer's manual.

99 2.7 *Oxygen radical absorbance capacity (ORAC) assay*

100 The free radical-scavenging activity of MK-4 was examined using ORAC assays. All
101 procedures were performed according to a previously published protocol [7]. In brief, a
102 mixture consisting of 20 μL of Trolox or samples in 75 mM phosphate buffer (pH 7.4),
103 200 μL of 9.44×10^{-8} M fluorescein solution, and 75 μL of 3.17×10^{-2} M AAPH solution
104 was incubated at 37°C for 1.5 h. To measure the ORAC values, phosphate buffer (75
105 mM) was used as a blank and Trolox solutions (6.25–50 μM) were used as standards. The

106 ORAC values of the samples were calculated using a Trolox standard curve. The relative
107 ORAC value [Trolox equivalents (TE)] was calculated as follows: relative ORAC value
108 = molarity of Trolox/molarity of the sample. Chlorogenic acid (CGA) was used as a
109 positive control.

110 *2.8 Nrf2 reporter gene assay*

111 The ability of MK-4 to activate Nrf2-dependent pathways was examined using reporter
112 gene assays. Cells were cultured in 96-well plates and incubated overnight, after which
113 the medium was replaced with Opti-MEM (Gibco, Carlsbad, CA, USA) containing
114 plasmids and Lipofectamine 3000 reagent (Thermo Fisher Scientific). The pGL4.37
115 plasmid harboring the firefly luciferase gene under the control of an antioxidant response
116 element (ARE) and the pGL4.75 plasmid containing the *Renilla* luciferase gene were used
117 as internal controls. After incubation for 24 h, fresh medium containing MK-4 was added
118 and the cells were incubated for another 24 h. A Dual-Glo Luciferase Reporter Assay
119 System (Promega, Madison, WI, USA) was used according to the manufacturer's
120 instructions. Firefly and Renilla luminescence were measured using a Wallac 1420
121 ARVO Mx plate reader (PerkinElmer).

122 2.9 *Mitochondrial ROS levels*

123 HK-2 cells were cultured in black 96-well plates, and mitochondrial ROS production
124 was measured using the ROS indicator dihydrorhodamine 123 (DHR123), a non-
125 fluorescent dye that is oxidized to rhodamine 123, a fluorescent dye that localizes to the
126 mitochondria [8]. Cells were incubated with 5 μM DHR123 in DMEM (FBS-free) for 20
127 min at 37°C. Fluorescence (excitation/emission: 485/535 nm) was measured using a
128 Wallac 1420 ARVO Mx plate reader (PerkinElmer).

129 *2.10 Microscopy imaging and quantitative analysis of mitochondrial morphology*

130 HK-2 cells were cultured in 35-mm dishes and stained with a mixture of 5 μg/mL
131 Hoechst33342 (Dojindo) and 0.1 μM MitoTracker green (Invitrogen) for nuclei and
132 mitochondria, respectively. After 20 min incubation at 37°C, images were captured using
133 a BZ-9000 all-in-one fluorescence microscope (Keyence, Osaka, Japan). A quantitative
134 assessment of Mitochondrial morphology was evaluated by employing the Mitochondrial
135 Network Analysis toolset, which is part of the existing ImageJ plug-ins, following the
136 analysis described by Valente *et al* [9].

137 *2.11 Protein expression levels*

HK-2 cells were cultured in 6-well plates overnight, followed by the addition of BSO and MK-4 and incubation for a further 36 h. After cell lysis, protein concentrations were determined using a Pierce™ BCA Protein Assay Kit (Thermo Fisher Scientific, Waltham, MA, USA). Equal amounts of protein (20 μg) were separated on a 5–20% SDS-PAGE gel (Atto, Tokyo, Japan) and transferred onto a 0.2 μm polyvinylidene difluoride membrane (Millipore, Bedford, MA, USA). The membrane was blocked against non-specific reactions with 5% BSA in Tris-buffered saline with 0.1% Tween 20 (TBS-T) for 1 hour at room temperature. Thereafter, the membranes were incubated overnight at 4 °C with primary antibodies specific to DRP1 (1:1,000, sc-271583, Santa Cruz Biotechnology, Dallas, TX, USA), FIS1 (1:1,000, sc-376447, Santa Cruz Biotechnology), and β-actin (1:1,000, M177-3, MBL Co., Ltd., Nagoya, Japan). After washing with TBS-T, incubated with HRP-conjugated secondary antibodies (1:10,000) for 1 hour at room temperature. The stained bands were visualized using an enhanced chemiluminescence (ECL) detection system (Atto). Images were captured and documented using a CCD system (ChemiDocTM MP Imaging System, Bio-Rad, Hercules, CA, USA). The relative expression level of each protein was normalized to that of β-actin.

154 *2.12 Lactate levels*

155 HK-2 cells were cultured in 12-well plates overnight, followed by the addition of BSO
156 and MK-4 and incubation for a further 36 h. Lactate levels in the culture medium were
157 measured using a Lactate Assay Kit-WST (Dojindo). Absorbance was measured at 450
158 nm using a Wallac 1420 ARVO Mx plate reader (PerkinElmer).

159 *2.13 Oxygen consumption rate (OCR) measurement*

160 To assess the function of mitochondrial oxidative phosphorylation (OXPHOS), the
161 mitochondrial OCR of HK-2 cells with BSO and/or MK-4 treatments were measured
162 using XFp mini-plates and a XFp extracellular flux analyzer (Agilent, Santa Clara, CA,
163 USA). For oxidative stress stimulation, the cells were cultured in a mini-plate and treated
164 with BSO and MK-4 in DMEM (without phenol red) for an additional 36 h. For the non-
165 oxidative-stress condition, the cells were treated with MK-4 alone in DMEM for 8 h.
166 Mitochondrial OXPHOS function was then assessed using the Mito Stress Test Kit
167 (without phenol red), with injections of oligomycin (2 μM), FCCP [carbonyl cyanide 4-
168 (trifluoromethoxy)phenylhydrazone, 1 μM], and a cocktail of rotenone/antimycin A (0.25

169 μM). Multiple parameters for mitochondrial respiratory capacity were assessed in this
170 assay [10].

171 *2.14 Mitochondrial DNA (mtDNA) copy number measurement*

172 HK-2 cells were cultured in six-well plates overnight, followed by the addition of MK-
173 4 and incubation for an additional 8 h. DNA was isolated using a NucleoSpin® Tissue
174 kit (TaKaRa Bio Inc.) according to the manufacturer's instructions. The mtDNA copy
175 number in the cells under MK-4 treatment was estimated using qRT-PCR and the Human
176 Mitochondrial DNA Monitoring Primer Set (TaKaRa Bio Inc.), which included the
177 mitochondrial genes NADH dehydrogenase subunit 1 (*ND1*) and *ND5*, as well as the
178 nuclear genes (nDNA) *SLCO2B1*, and *SERPINA1*. mtDNA levels were normalized to
179 nDNA levels, following the manufacturer's protocol.

180 *2.15 Statistical analysis*

181 The data are expressed as the mean ± standard deviation. The data in Figure 1A, 1B,
182 2D, 3A, 3B, 4B, 6D, 7C, and 7D were analyzed using one-way analysis of variance
183 (ANOVA), followed by Tukey's post hoc test. The time-course data (Figure 1C and 5A–
184 C) and inhibitor data (Figure 2A, 2B, 2E, 4A, and 6A) were analyzed using two-way

ANOVA followed by Tukey's post hoc test. Data from 7B were analyzed using unpaired Student's t-tests. Statistical analyses were performed using GraphPad Prism version 10.2.3 (GraphPad Software, San Diego, CA, USA). p values of <0.05 were considered significant.

3. Results and Discussion

3.1 MK-4 prevented BSO-induced cell death in HK-2 cells

In this study, BSO was used to inhibit the activity of γ-glutamylcysteine synthetase and deplete cellular antioxidant (GSH) levels, inducing oxidative stress and the death of HK-2 cells [11-12]. In our preliminary experiments, we found that concentrations below 30 μM of BSO failed to induce cytotoxicity (Figure S1). To assess the protective effect of MK-4 in BSO-induced HK-2 cells, the cells were co-treated with 100 μM BSO and 0.001–1.0 μM MK-4 for 48 h. Cell viability and cytotoxicity were then measured (Figure 1A and 1B). The addition of 100 μM BSO resulted in significant cell death and high cytotoxicity in HK-2 cells, whereas MK-4 increased cell viability and reduced cytotoxicity in a dose-dependent manner. To confirm the damage to HK-2 cells, we examined the mRNA

201 expression levels of *KIM-1*, *ENDOG*, and *BIK* after BSO and MK-4 treatment for 12 and
202 36 h. KIM-1 is a well-established marker of renal tubular injury [13], while BIK and
203 ENDOG are associated with apoptotic cell death [14]. Our findings revealed that MK-4
204 decreased *KIM-1*, *BIK*, and *ENDOG* mRNA expression level in HK-2 cells with BSO
205 treatment (Figure 1C), suggesting that MK-4 protected the cells from BSO-induced cell
206 death.

207 To investigate the cytoprotective effects of MK-4 in HK-2 cells treated with BSO, we
208 measured MDA levels in the cells. MDA is a byproduct of lipid peroxidation and a marker
209 of oxidative stress [6]. The results showed that MK-4 reduced MDA levels in BSO-treated
210 cells (Figure 2A), indicating that it inhibited lipid peroxidation in response to oxidative
211 stress. Second, since BSO causes GSH disruption in cells [15], we also assessed the
212 GSH/GSSG ratio (Figure 2B). The GSH/GSSG ratio is an indicator of the oxidative stress
213 status and level of DNA damage [16]. The results showed that the GSH/GSSG ratio
214 decreased at 3 h and became remarkably low at 24 h. However, MK-4 did not affect the
215 GSH/GSSG ratio. This indicated that MK-4 improved cell viability without enhancing
216 GSH generation.

To confirm the antioxidant effects of MK-4 on HK-2 cells, we measured its direct and indirect antioxidant properties. Direct antioxidants are free radical scavengers that are sacrificed in the process of their antioxidant actions and need to be regenerated, whereas indirect antioxidants may not be redox active, but rather, they activate antioxidative pathways, including the ARE/Nrf2/KEAP-dependent pathway, which results in the transcriptional induction of cytoprotective proteins [17]. The ORAC assay is a common method for determining antioxidant capacity. The ARE-reporter gene assay, a tool used to study the ARE/Nrf2/KEAP-dependent antioxidant pathway, was performed to assessing direct and indirect antioxidant properties, respectively, of MK-4. The results showed that MK-4 has neither a direct free radical scavenging property (Figure 2C) nor an indirect antioxidant property of activation of the ARE/Nrf2/KEAP-related pathway (Figure 2D). This result revealed that MK-4 did not show direct or indirect antioxidant properties by scavenging free radicals or activating the ARE/Nrf2/KEAP-dependent antioxidant pathway in HK-2 cells.

The VK cycle has a potent antioxidant effect because it contains vitamin K-hydroquinone, a strong radical scavenger [18]. VK oxidoreductase (VKOR) is considered a

key enzyme in the VK cycle; however, a recent study revealed that ferroptosis suppressor protein 1 (FSP1, a ubiquinone oxidoreductase) also regulates the non-canonical VK cycle to inhibit ferroptosis [19]. Since BSO is considered a ferroptosis inducer, we also assessed the effects of MK-4 on ferroptosis and the VK cycle in HK-2 cells (Figure 2E). ML162, a GPx4 inhibitor, was used to induce ferroptosis [20], whereas warfarin (War) and iFSP1 are inhibitors of the VK cycle, inhibiting VKOR [21] and FSP1 [22], respectively. The results revealed that MK-4 showed cytoprotective effects without the regulation of GPx4 activation or the warfarin-dependent VK cycle by ML162 and warfarin, respectively. However, partial effects of MK-4 were abolished by iFSP1. This is in agreement with the results showing that FSP1 regulates the VK cycle to inhibit ferroptosis [19]. It is worth mentioning that, although the cytoprotective effects of MK-4 diminished with iFSP1 treatment, iFSP did not abolish all of its cytoprotective effects (cell viability remained 42.7% in cells with ML162, iFSP1, and MK-4 treatments).

3.2 MK-4 improved mitochondrial morphology by regulating mitochondrial quality in HK-2 cells treated with BSO

249 Previous studies have shown that apoptotic cell death induced by BIK and the
250 ENDOG-mediated pathway is related to mitochondrial function [23-24]. Mitochondria play
251 a central role in maintaining cell integrity, including the regulation of programmed cell
252 death and energy production [25]. As shown in Figure 1C, the mRNA expression levels of
253 *BIK* and *ENDOG* decreased in cells following BSO and MK-4 treatments. This suggested
254 that MK-4 protects mitochondria from oxidative stress. Given that ROS accumulation
255 leads to oxidative stress and that mitochondria are the primary sites of ROS production
256 [26], we measured mitochondrial ROS levels and mitochondrial morphology in the cells.
257 Excessive mitochondrial ROS levels were detected in HK-2 cells treated with BSO,
258 indicating the occurrence of oxidative stress (Figure 3A). Mitochondria with spherical
259 morphologies and low mitochondrial mean length were observed in cells treated with
260 BSO (Figure 3B). In contrast, low mitochondrial ROS levels and normal mitochondrial
261 morphology were observed in MK-4-treated cells (Figure 3A and 3B).
262 Moreover, cells with an increased proportion of mitochondrial networks show an
263 increase in the controllability, efficiency, and robustness of mitochondria, which
264 enhances their oxidative capacity [27]. The mitochondrial network features indicated that

265 the proportions of punctate and rod-shaped (individuals) mitochondria were 17.39% and
266 61.51% (sum of individuals were 78.90%) in the control group, 25.93% and 55.17% (sum
267 81.10%) in the BSO group, 19.94% and 56.81% (sum 76.75%) in the MK-4 (0.1 μM) +
268 BSO group, and 19.13% and 54.94% (sum 74.07%) in the MK-4 (1 μM) + BSO group
269 (Figure 3C). Moreover, the mitochondrial networks proportions were 21.10% in the
270 control group, 18.90% in the BSO group, 23.24% in the MK-4 (0.1 μM) + BSO group,
271 and 25.93% in the MK-4 (1 μM) + BSO group (Figure 3C). This suggests that BSO
272 induces mitochondrial ROS production and mitochondrial fragmentation, whereas MK-4
273 ameliorates the BSO-induced mitochondrial damage.

274 Oxidative stress causes mitochondrial spherical morphology and fragmentation, which
275 are linked to the induction of mitochondrial-dependent apoptosis [28]. Taken together, our
276 results suggested that MK-4 protected cell through maintenance of mitochondrial
277 function to avoid cell death. Mechanisms that contribute to mitochondrial quality control
278 include mitochondrial fusion and fission and mitophagy [27,29]. Because mitochondrial
279 fragmentation is mainly regulated by mitochondrial fission, we further measured the
280 expression of the mitochondrial fission-related genes, *DRP1* and *FIS1,* which are core

proteins that modulate mitochondrial morphology [30-31]. The expression levels of *DRP1* and *FIS1* increased in cells treated with BSO, whereas MK-4 treatment reduced the expression levels of these genes (Figure 4A). Moreover, the protein expression level of DRP1 also increased in cells treated with BSO, whereas MK-4 treatment reduced its expression levels (Figure 4B). It suggested that mitochondrial fragmentation was enhanced by oxidative stress and that MK-4 inhibited mitochondrial fission. Although the protein expression level of FIS1 did not show a significant change in this study, studies suggested that DRP1/FIS1-mediated mitochondrial fission play an important mechanism of pathologic alterations in mitochondrial morphology [32], further studies will be necessary to confirm these findings. These results indicated that oxidative stress causes mitochondrial fragmentation, whereas MK-4 improves the balance of mitochondrial dynamics, resulting in better mitochondrial morphology.

3.3 MK-4 inhibits autophagy/mitophagy to protect BSO-treated cells from mitochondrial breakdown and cell death

296 The autophagic activity is a critical process for preserving cellular integrity. Oxidative
297 stress serves as the main intracellular signaling transducers sustaining autophagy [33-34].
298 Damaged organelles are enclosed by double-membrane vesicles called autophagosomes,
299 which are subsequently degraded by lysosomes [35-36]. Autophagosomes are formed
300 through a multistep process, p62 is a receptor that directly binds to LC3 and GABARAP
301 family proteins, promoting the delivery of cargo to the autophagosomes and lysosomes
302 degradation [35-36]. In this study, *GABARAPL1*, *SQSTM1*/*p62*, and *LC3B* levels were
303 increased in cells under BSO treatment. However, treatment with MK-4 decreased the
304 expression levels of these genes (Figure 5A). Thus, MK-4 inhibits autophagic flux to
305 protect cells from autophagic cell death.
306 Removal of abnormal mitochondria is an essential process in mitophagy, a form of
307 selective autophagy. It can be broadly categorized into ubiquitin- and receptor-mediated
308 mitophagy [37]. We determined the expression levels of the genes related to ubiquitin- and
309 receptor-mediated mitophagy to elucidate the effects of MK-4 on elimination of
310 dysfunctional mitochondria. BSO addition increased the expression levels of ubiquitin-

311 mediated (Figure 5B) and receptor-mediated (Figure 5C) mRNA in the cells, MK-4
312 inhibited both ubiquitin- and receptor-mediated mitophagy-related gene expression.
313 Ubiquitin-mediated mitophagy is commonly facilitated by the Pink1/Parkin pathway
314 and receptor-mediated mitophagy, in which a membrane/cargo-bound receptor is
315 activated, which then interacts directly with autophagosomal marker proteins [38-39].
316 Ubiquitin-mediated mitophagy plays a major role in the elimination of dysfunctional
317 mitochondria. Pink1 acts as a signal-amplifying protein in phosphorylates ubiquitin, and
318 phospho-ubiquitin on mitophagy [39]. Furthermore, receptors locate on the outer
319 mitochondrial membrane also play a critical role in mitophagy, a primary pathway
320 responsible for targeting mitochondria [38, 40-42]. Taken together, these results revealed that
321 BSO induces excessive mitochondrial ROS production and autophagic activity, resulting
322 in mitochondrial breakdown and cell death. Despite this, MK-4 inhibited mitochondrial
323 breakdown by regulating mitophagy, which is related to mitochondrial quantity control.
324
325 *3.4 MK-4 regulated mitochondrial function in BSO-induced oxidative damage*

326 Based on these results, energy metabolism may also change in cells under BSO and
327 MK-4 treatments. The intracellular lactate level was assessed as a biomarker of
328 mitochondrial dysfunction. Abnormal mitochondrial OXPHOS results in a shift toward
329 anaerobic respiration and lactate production [43]. We found that intracellular lactate levels
330 increased in cells after BSO treatment; however, MK-4 decreased lactate levels in these
331 cells (Figure 6A). Next, we determined the oxygen consumption rate (OCR) for assessing
332 mitochondrial OXPHOS function. A mitochondrial stress assay was used to determine
333 the parameters of mitochondrial OXPHOS (Figure 6B). In brief, basal respiration was
334 measured without any stimulators or inhibitors, oligomycin was added to inhibit ATP
335 synthase for ATP-linked respiration, FCCP was added to uncouple the mitochondria for
336 maximal respiration, a cocktail of rotenone/antimycin A (inhibitors of OXPHOS
337 complexes I and III) was added to inhibit OXPHOS, and the remaining OCR indicated
338 non-mitochondrial respiration (Figure 6B and C). Proton leak-linked respiration refers to
339 mitochondrial inefficiency, in which the remaining basal respiration is not coupled to
340 ATP production [44]. The results showed that although all parameters were significantly
341 decreased in HK-2 cells treated with BSO, the addition of MK-4 maintained all

parameters, including basal, ATP-linked, maximal, proton leak-linked, and non-mitochondrial respiration (Figure 6C). The increased OCR may reflect both improved mitochondrial function and enhanced cell survival in the cells with MK-4 treatment. This suggested that mitochondrial function was preserved by the addition of MK-4 to protect the cells before the mitochondria were destroyed by oxidative stress.

3.5 MK-4 regulated mitochondrial function without oxidative stress stimulation

We also measured energy metabolism in MK-4-treated cells without oxidative stress stimulation. The results showed that the addition of MK-4 increased ATP-linked and maximal respiration (Figure 7A and 7B), suggesting that MK-4 enhanced mitochondrial oxidative phosphorylation. Consistent with this result, MK-4 also increased intracellular ATP levels (Figure 7C). Moreover, a previous study indicated that MK-4 improves ATP production and respiration at low concentrations, but can be harmful at higher levels (10 μM) in porcine intestinal epithelial cells [45]. However, MK-4 protected mitochondrial function without causing toxicity to HK-2 cells (Figure S2). Of note, we also found that MK-4 did not increase the mtDNA copy number (Figure 7D), suggesting that it may

358 enhance mitochondrial function (quality), but not mitochondrial content. Despite its
359 structural similarity to coenzyme Q10 (CoQ10), VK2 does not function as a viable
360 substitute for CoQ10 in the mitochondrial energy metabolism of mammalian cells [46]. Here,
361 we found that MK-4 enhanced mitochondrial oxidative phosphorylation in HK-2 cells,
362 indicating that MK-4 may regulate other key factors involved in ATP production. Certain
363 limitations should be noted in this study. As the experiments were conducted using a cell-
364 based model, they may not cover the full complexity of mitochondrial function in vivo,
365 and thus may not entirely reflect the physiological processes occurring in the kidney.
366 Moreover, as phylloquinone and MK-7, other biologically active forms of vitamin K, are
367 also commonly studied for their potential effects compared with MK-4 [47-48], further
368 studies are needed to confirm whether MK-4 and other subtypes exert beneficial effects
369 in nephropathy mice models.

370 In conclusion, this study showed that MK-4 improved mitochondrial quantity by
371 regulating mitochondrial ROS production and mitochondrial dynamics in HK-2 cells
372 under oxidative stress; furthermore, MK-4 also enhanced ATP production by regulating
373 mitochondrial oxidative phosphorylation. These results showed the possibility that MK-

374 4 prevents renal diseases by acting on proximal tubule cells, which has beneficial effects

375 on mitochondrial function.

376

377 **Abbreviations**

378 ARE: antioxidant response element

379 ANOVA: analysis of variance

380 BSO: L-buthionine-(S, R)-sulfoximine

381 CGA: chlorogenic acid

382 DHMBA: 3,5-dihydroxy-4-methoxybenzyl alcohol

383 DHR123: dihydrorhodamine 123

384 DMEM: Dulbecco's modified Eagle's medium

385 FBS: fetal bovine serum

386 FCCP: carbonyl cyanide 4-(trifluoromethoxy)phenylhydrazone

387 FSP1: ferroptosis suppressor protein 1

388 GSH: glutathione

389 MDA: malondialdehyde

MK-4: menaquinone-4

mtDNA: mitochondrial DNA

ND1 &5: NADH dehydrogenase subunit 1 and 5

nDNA: nuclear DNA

OCR: oxygen consumption rate

ORAC: oxygen radical absorbance capacity

OXPHOS: oxidative phosphorylation

qRT-PCR: quantitative reverse transcription polymerase chain reaction

ROS: reactive oxygen species

TBARS: thiobarbituric-acid-reactive substance

TE: Trolox equivalents

VK: vitamin K

VKOR: VK oxidoreductase

War: warfarin

AUTHOR INFORMATION

Corresponding Authors

Shu-Ping Hui - Faculty of Health Sciences, Hokkaido University, Kita 12, Nishi 5, Kita-ku, Sapporo, Sapporo 060-0812, Japan; Tel.: +81-11-706-3693; ORCiD https://orcid.org/0000-0001-9973-6461. Email: keino@hs.hokudai.ac.jp

Authors

Hsinjung Ho - Faculty of Health Sciences, Hokkaido University, Kita 12, Nishi 5, Kita-ku, Sapporo, Sapporo 060-0812, Japan. ORCiD https://orcid.org/0000-0001-8421-4919.

Natsumi Aoki - Faculty of Health Sciences, Hokkaido University, Kita 12, Nishi 5, Kita-ku, Sapporo, Sapporo 060-0812, Japan.

Miki Eguchi - Faculty of Health Sciences, Hokkaido University, Kita 12, Nishi 5, Kita-ku, Sapporo, Sapporo 060-0812, Japan.

Mingchen Gao - Faculty of Health Sciences, Hokkaido University, Kita 12, Nishi 5, Kita-ku, Sapporo, Sapporo 060-0812, Japan.

Hirotaka Suzuki- Faculty of Health Sciences, Hokkaido University, Kita 12, Nishi 5, Kita-ku, Sapporo, Sapporo 060-0812, Japan.

Mao Mikami- Faculty of Health Sciences, Hokkaido University, Kita 12, Nishi 5, Kita-ku, Sapporo, Sapporo 060-0812, Japan.

Hitoshi Chiba - Faculty of Health Sciences, Hokkaido University, Kita 12, Nishi 5, Kita-ku, Sapporo, Sapporo 060-0812, Japan; Department of Nutrition, Sapporo University of Health Sciences, Nakanuma Nishi-4-2-1-15, Higashi-ku, Sapporo 007-0894, Japan.

Notes

429 The authors declare no competing financial interest.

430

431 **Data Availability**

432 Data will be made available on request.

433

434 **Funding**

435 This work was partially supported by a Grant-in-aid for Scientific Research from the

436 Japan Society for the Promotion of Science (JSPS) to H-J H (20K1966800 and

437 22K1174602).

438

439 **Conflicts of interest**

440 The authors declare no conflicts of interest.

References

1. Khand, F. D.; Gordge, M. P.; Robertson, W. G.; Noronha-Dutra, A. A.; Hothersall, J. S., Mitochondrial superoxide production during oxalate-mediated oxidative stress in renal epithelial cells. *Free radical biology & medicine* **2002,** *32 12*, 1339-50.
2. Tirichen, H.; Yaigoub, H.; Xu, W.; Wu, C.; Li, R.; Li, Y., Mitochondrial Reactive Oxygen Species and Their Contribution in Chronic Kidney Disease Progression Through Oxidative Stress. *Front Physiol* **2021,** *12*, 627837.
3. Martius, C.; Alvino, C., [ON THE TRANSFORMATION OF VITAMIN K-1 (PHYLLOCHINON) INTO VITAMIN K2(20) BY THE DEVELOPMENT OF AN EMBRYO IN A HEN'S EGG]. *Biochem Z* **1964,** *340*, 316-9.
4. Ivanova, D.; Zhelev, Z.; Getsov, P.; Nikolova, B.; Aoki, I.; Higashi, T.; Bakalova, R., Vitamin K: Redox-modulation, prevention of mitochondrial dysfunction and anticancer effect. *Redox Biol* **2018,** *16*, 352-358.
5. Muszyńska, M.; Ambrożewicz, E.; Gęgotek, A.; Grynkiewicz, G.; Skrzydlewska, E., Protective Effects of Vitamin K Compounds on the Proteomic Profile of Osteoblasts under Oxidative Stress Conditions. *Molecules* **2020,** *25* (8).
6. Aguilar Diaz De Leon, J.; Borges, C. R., Evaluation of Oxidative Stress in Biological Samples Using the Thiobarbituric Acid Reactive Substances Assay. *J Vis Exp* **2020,** (159).
7. Watanabe, M.; Fuda, H.; Jin, S.; Sakurai, T.; Hui, S. P.; Takeda, S.; Watanabe, T.; Koike, T.; Chiba, H., A phenolic antioxidant from the Pacific oyster (Crassostrea gigas) inhibits oxidation of cultured human hepatocytes mediated by diphenyl-1-pyrenylphosphine. *Food Chem* **2012,** *134* (4), 2086-9.
8. Cheng, J.; Park, T. S.; Chio, L. C.; Fischl, A. S.; Ye, X. S., Induction of apoptosis by sphingoid long-chain bases in Aspergillus nidulans. *Mol Cell Biol* **2003,** *23* (1), 163-77.
9. Valente, A. J.; Maddalena, L. A.; Robb, E. L.; Moradi, F.; Stuart, J. A., A simple ImageJ macro tool for analyzing mitochondrial network morphology in mammalian cell culture. *Acta Histochem* **2017,** *119* (3), 315-326.
10. Ho, H. J.; Aoki, N.; Wu, Y. J.; Gao, M. C.; Sekine, K.; Sakurai, T.; Chiba, H.; Watanabe, H.; Watanabe, M.; Hui, S. P., A Pacific Oyster-Derived Antioxidant, DHMBA, Protects Renal Tubular HK-2 Cells against Oxidative Stress via Reduction of

Mitochondrial ROS Production and Fragmentation. *Int J Mol Sci* **2023,** *24* (12).
11. Anderson, C. P.; Tsai, J. M.; Meek, W. E.; Liu, R. M.; Tang, Y.; Forman, H. J.; Reynolds, C. P., Depletion of glutathione by buthionine sulfoxine is cytotoxic for human neuroblastoma cell lines via apoptosis. *Exp Cell Res* **1999,** *246* (1), 183-92.
12. Chen, J.; Small-Howard, A.; Yin, A.; Berry, M. J., The responses of Ht22 cells to oxidative stress induced by buthionine sulfoximine (BSO). *BMC Neurosci* **2005,** *6*, 10.
13. Yin, C.; Wang, N., Kidney injury molecule-1 in kidney disease. *Ren Fail* **2016,** *38* (10), 1567-1573.
14. Wang, C.; Youle, R. J., The role of mitochondria in apoptosis*. *Annu Rev Genet* **2009,** *43*, 95-118.
15. Friesen, C.; Kiess, Y.; Debatin, K. M., A critical role of glutathione in determining apoptosis sensitivity and resistance in leukemia cells. *Cell Death & Differentiation* **2004,** *11* (1), S73-S85.
16. Asensi, M.; Sastre, J.; Pallardo, F. V.; Lloret, A.; Lehner, M.; Garcia-de-la Asuncion, J.; Viña, J., [23] Ratio of reduced to oxidized glutathione as indicator of oxidative stress status and DNA damage. In *Methods in Enzymology*, Academic Press: 1999; Vol. 299, pp 267-276.
17. Dinkova-Kostova, A. T.; Talalay, P., Direct and indirect antioxidant properties of inducers of cytoprotective proteins. *Mol Nutr Food Res* **2008,** *52 Suppl 1*, S128-38.
18. Vervoort, L. M. T.; Ronden, J. E.; Thijssen, H. H. W., The potent antioxidant activity of the vitamin K cycle in microsomal lipid peroxidation. *Biochemical Pharmacology* **1997,** *54* (8), 871-876.
19. Mishima, E.; Ito, J.; Wu, Z.; Nakamura, T.; Wahida, A.; Doll, S.; Tonnus, W.; Nepachalovich, P.; Eggenhofer, E.; Aldrovandi, M.; Henkelmann, B.; Yamada, K.-i.; Wanninger, J.; Zilka, O.; Sato, E.; Feederle, R.; Hass, D.; Maida, A.; Mourão, A. S. D.; Linkermann, A.; Geissler, E. K.; Nakagawa, K.; Abe, T.; Fedorova, M.; Proneth, B.; Pratt, D. A.; Conrad, M., A non-canonical vitamin K cycle is a potent ferroptosis suppressor. *Nature* **2022,** *608* (7924), 778-783.
20. Moosmayer, D.; Hilpmann, A.; Hoffmann, J.; Schnirch, L.; Zimmermann, K.; Badock, V.; Furst, L.; Eaton, J. K.; Viswanathan, V. S.; Schreiber, S. L.; Gradl, S.; Hillig, R. C., Crystal structures of the selenoprotein glutathione peroxidase 4 in its apo form and in complex with the covalently bound inhibitor ML162. *Acta Crystallogr D Struct Biol* **2021,** *77* (Pt 2), 237-248.

21. Rishavy, M. A.; Hallgren, K. W.; Wilson, L.; Singh, S.; Runge, K. W.; Berkner, K. L., Warfarin alters vitamin K metabolism: a surprising mechanism of VKORC1 uncoupling necessitates an additional reductase. *Blood* **2018,** *131* (25), 2826-2835.
22. Doll, S.; Freitas, F. P.; Shah, R.; Aldrovandi, M.; da Silva, M. C.; Ingold, I.; Goya Grocin, A.; Xavier da Silva, T. N.; Panzilius, E.; Scheel, C. H.; Mourão, A.; Buday, K.; Sato, M.; Wanninger, J.; Vignane, T.; Mohana, V.; Rehberg, M.; Flatley, A.; Schepers, A.; Kurz, A.; White, D.; Sauer, M.; Sattler, M.; Tate, E. W.; Schmitz, W.; Schulze, A.; O'Donnell, V.; Proneth, B.; Popowicz, G. M.; Pratt, D. A.; Angeli, J. P. F.; Conrad, M., FSP1 is a glutathione-independent ferroptosis suppressor. *Nature* **2019,** *575* (7784), 693-698.
23. Yang, S. H.; Chien, C. M.; Lu, M. C.; Lin, Y. H.; Hu, X. W.; Lin, S. R., Up-regulation of Bax and endonuclease G, and down-modulation of Bcl-XL involved in cardiotoxin III-induced apoptosis in K562 cells. *Exp Mol Med* **2006,** *38* (4), 435-44.
24. Kutuk, O.; Aytan, N.; Karakas, B.; Kurt, A. G.; Acikbas, U.; Temel, S. G.; Basaga, H., Biphasic ROS production, p53 and BIK dictate the mode of cell death in response to DNA damage in colon cancer cells. *PLoS One* **2017,** *12* (8), e0182809.
25. Supinski, G. S.; Schroder, E. A.; Callahan, L. A., Mitochondria and Critical Illness. *Chest* **2020,** *157* (2), 310-322.
26. Bandy, B.; Davison, A. J., Mitochondrial mutations may increase oxidative stress: implications for carcinogenesis and aging? *Free Radic Biol Med* **1990,** *8* (6), 523-39.
27. Hoitzing, H.; Johnston, I. G.; Jones, N. S., What is the function of mitochondrial networks? A theoretical assessment of hypotheses and proposal for future research. *Bioessays* **2015,** *37* (6), 687-700.
28. Willems, P. H.; Rossignol, R.; Dieteren, C. E.; Murphy, M. P.; Koopman, W. J., Redox Homeostasis and Mitochondrial Dynamics. *Cell Metab* **2015,** *22* (2), 207-18.
29. Ho, H. J.; Shirakawa, H.; Yoshida, R.; Ito, A.; Maeda, M.; Goto, T.; Komai, M., Geranylgeraniol enhances testosterone production via the cAMP/protein kinase A pathway in testis-derived I-10 tumor cells. *Bioscience, biotechnology, and biochemistry* **2016,** *80* (4), 791-7.
30. Twig, G.; Shirihai, O. S., The interplay between mitochondrial dynamics and mitophagy. *Antioxid Redox Signal* **2011,** *14* (10), 1939-51.
31. Picard, M.; Shirihai, O. S.; Gentil, B. J.; Burelle, Y., Mitochondrial morphology

539 transitions and functions: implications for retrograde signaling? *Am J Physiol Regul*
540 *Integr Comp Physiol* **2013,** *304* (6), R393-406.
541 32. Haileselassie, B.; Mukherjee, R.; Joshi, A. U.; Napier, B. A.; Massis, L. M.;
542 Ostberg, N. P.; Queliconi,B. B.; Monack, D.; Bernstein, D.; Mochly-Rosen, D., Drp1/Fis1
543 interaction mediates mitochondrial dysfunction in septic cardiomyopathy. *J Mol Cell*
544 *Cardiol* **2019,** *130*, 160-169.
545 33. Glick, D.; Barth, S.; Macleod, K. F., Autophagy: cellular and molecular
546 mechanisms. *J Pathol* **2010,** *221* (1), 3-12.
547 34. Yun, H. R.; Jo, Y. H.; Kim, J.; Shin, Y.; Kim, S. S.; Choi, T. G., Roles of
548 Autophagy in Oxidative Stress. *Int J Mol Sci* **2020,** *21* (9).
549 35. Tanida, I.; Minematsu-Ikeguchi, N.; Ueno, T.; Kominami, E., Lysosomal
550 turnover, but not a cellular level, of endogenous LC3 is a marker for autophagy.
551 *Autophagy* **2005,** *1* (2), 84-91.
552 36. Yoshii, S. R.; Mizushima, N., Monitoring and Measuring Autophagy. *Int J Mol*
553 *Sci* **2017,** *18* (9).
554 37. Sulkshane, P.; Ram, J.; Thakur, A.; Reis, N.; Kleifeld, O.; Glickman, M. H.,
555 Ubiquitination and receptor-mediated mitophagy converge to eliminate oxidation-
556 damaged mitochondria during hypoxia. *Redox Biol* **2021,** *45*, 102047.
557 38. Yamaguchi, O.; Murakawa, T.; Nishida, K.; Otsu, K., Receptor-mediated
558 mitophagy. *J Mol Cell Cardiol* **2016,** *95*, 50-6.
559 39. Zimmermann, M.; Reichert, A. S., How to get rid of mitochondria: crosstalk
560 and regulation of multiple mitophagy pathways. *Biological Chemistry* **2018,** *399* (1), 29-
561 45.
562 40. Liu, L.; Feng, D.; Chen, G.; Chen, M.; Zheng, Q.; Song, P.; Ma, Q.; Zhu, C.;
563 Wang, R.; Qi, W.; Huang, L.; Xue, P.; Li, B.; Wang, X.; Jin, H.; Wang, J.; Yang, F.; Liu,
564 P.; Zhu, Y.; Sui, S.; Chen, Q., Mitochondrial outer-membrane protein FUNDC1 mediates
565 hypoxia-induced mitophagy in mammalian cells. *Nat Cell Biol* **2012,** *14* (2), 177-85.
566 41. Feng, D.; Liu, L.; Zhu, Y.; Chen, Q., Molecular signaling toward mitophagy
567 and its physiological significance. *Exp Cell Res* **2013,** *319* (12), 1697-1705.
568 42. Liu, L.; Sakakibara, K.; Chen, Q.; Okamoto, K., Receptor-mediated mitophagy
569 in yeast and mammalian systems. *Cell Res* **2014,** *24* (7), 787-95.
570 43. Jeong, H.; Dimick, M. K.; Sultan, A.; Duong, A.; Park, S. S.; El Soufi El
571 Sabbagh, D.; Goldstein, B. I.; Andreazza, A. C., Peripheral biomarkers of mitochondrial

572 dysfunction in adolescents with bipolar disorder. *Journal of Psychiatric Research* **2020,**
573 *123*, 187-193.
574 44. Cheng, J.; Nanayakkara, G.; Shao, Y.; Cueto, R.; Wang, L.; Yang, W. Y.; Tian,
575 Y.; Wang, H.; Yang, X., Mitochondrial Proton Leak Plays a Critical Role in Pathogenesis
576 of Cardiovascular Diseases. *Adv Exp Med Biol* **2017,** *982*, 359-370.
577 45. Bernardini, C.; Algieri, C.; La Mantia, D.; Trombetti, F.; Pagliarani, A.; Forni,
578 M.; Nesci, S., Vitamin K Vitamers Differently Affect Energy Metabolism in IPEC-J2
579 Cells. *Front Mol Biosci* **2021,** *8*, 682191.
580 46. Cerqua, C.; Casarin, A.; Pierrel, F.; Vazquez Fonseca, L.; Viola, G.; Salviati, L.;
581 Trevisson, E., Vitamin K2 cannot substitute Coenzyme Q(10) as electron carrier in the
582 mitochondrial respiratory chain of mammalian cells. *Sci Rep* **2019,** *9* (1), 6553.
583 47. Okano, t.; Shimomura, Y.; Yamane, M.; Suhara, Y.; Kamao, M.; Sugiura, M.;
584 Nakagawa, K., Conversion of phylloquinone (Vitamin K1) into menaquinone-4 (Vitamin
585 K2) in mice: two possible routes for menaquinone-4 accumulation in cerebra of mice. *J*
586 *Biol Chem* **2008,** *283 (17)*, 11270-11279.
587 48 Shearer, M. J.; P Newman, P., Metabolism and cell biology of vitamin K.
588 *Thromb Haemost* **2008,** *100 (4)*, 530-547.
589

590

591 **Table**

592 **Table 1 List of primers**

Gene name	Primer (5'→3')	Accession No.
Damage marker		
KIM-1	F: 5'- GAAGTGGCTACTGGTTCATGG -3'	NM_001173393.3
	R: 5'- ACGACTGTTCGAACGAGCAC -3'	
BIK	F: 5'- GACCTGGACCCTATGGAGGAC -3'	NM_001197.5
	R: 5'- CCTCAGTCTGGTCGTAGATGA -3'	
ENDOG	F: 5'- AGCAGGTGGGCAAATTGAG -3'	NM_004435.2
	R: 5'- CCAGGATGTTTGGCACAAAGAG -3'	
Mitochondrial fission-related genes		
DRP1	F: 5'- CGCAATCCATCGGCGAGGAT -3'	NM_001278465.2
	R: 5'- ACCACAGGATAAGTCACCGAG -3'	
FIS1	F: 5'- TGAACTGAGGGACAGTGATTTC -3'	NM_016068.3
	R: 5'- CCCAAGGGTAGCTCAGTTTATC -3'	
Autophagy and mitophagy-related genes		
LC3B	F: 5'- ACCATGCCGTCGGAGAAGAC -3'	NM_001085481.3
	R: 5'- TCTCGAATAAGTCGGACATCTTCTACTCT -3'	
GABARAPL1	F: 5'- ATCGGAAAAAGGAAGGAGAAAAGATC -3'	NM_001363598.2
	R: 5'- CAGGCACCCTGGCTTTTGG -3'	
BNIP3	F: 5'- AGCGCCCGGGATGCA -3'	NM_004052.4
	R: 5'- CCCGTTCCCATTATTGCTGAA -3'	
BNIP3L	F: 5'- CTGCGAGGAAAATGAGCAGTCTCT -3'	NM_004331.3
	R: 5'- GCCCCCCATTTTTCCCATTG -3'	
FUNDC1	F: 5'- GAAACGAGCGAACAAAGCAG -3'	NM_173794.4
	R: 5'- GCAAAAAGCCTCCCACAAAT -3'	
PINK1	F: 5'- CGTTGGACACGAGACGCTTGCA -3'	NM_032409.3
	R: 5'- GCAATGTAGGCATGGTGGCTTCATAC -3'	
OPTN	F: 5'- AAGGAGCAACTGGCATTGCA -3'	NM_001008212.2
	R: 5'- TCTCCATCAAGGACTGCCTG -3'	
CALCOCO2	F: 5'- TCTTTGCCGTATCAAGTACCTACT -3'	NM_001261393.2

	R: 5'- GGCATTTCTTGATGGAGAGCG -3'	
House keeping gene		
β-actin	F: 5'- ATAGCACAGCCTGGATAGCAACGTAC -3'	NM_001101.5
	R: 5'- CACCTTCTACAATGAGCTGCGTGTG -3'	

593 F: Forward; R: Reverse.

594

595

Figure legends

Figure 1. Cytoprotective effects of MK-4 in HK-2 cells treated with BSO.

(A) Cell viability (n = 5–6). (B) Cytotoxicity (n = 5–6). (C) mRNA expression levels of damage markers (n = 3–4). MK-4, menaquinone-4; BSO, L-buthionine-(S,R)-sulfoximine. Values with different letters indicate significant differences at $p < 0.05$.

Figure 2. Antioxidative effects of MK-4 in HK-2 cells treated with BSO.

(A) Malondialdehyde (MDA) content (n = 3). (B) Glutathione (GSH)/oxidized GSH (GSSG) ratio (n = 4). (C) Oxygen radical absorbance capacity (ORAC) assay. CGA (Chlorogenic acid) was used as a positive control. (D) ARE/Nrf2/KEAP-related pathway (n = 5–6). PC: positive control. 500 μM DHMBA (3,5-dihydroxy-4-methoxybenzyl alcohol), a Nrf2 activator. (E) Cell viability after inhibitor treatments (n = 5–6). ML162: GPx4 inhibitor, War: VKOR inhibitor, iFSP1: FSP1 inhibitor. Values with different letters indicate significant differences at $p < 0.05$.

Figure 3. Effect of MK-4 on mitochondrial damage in HK-2 cells treated with BSO.

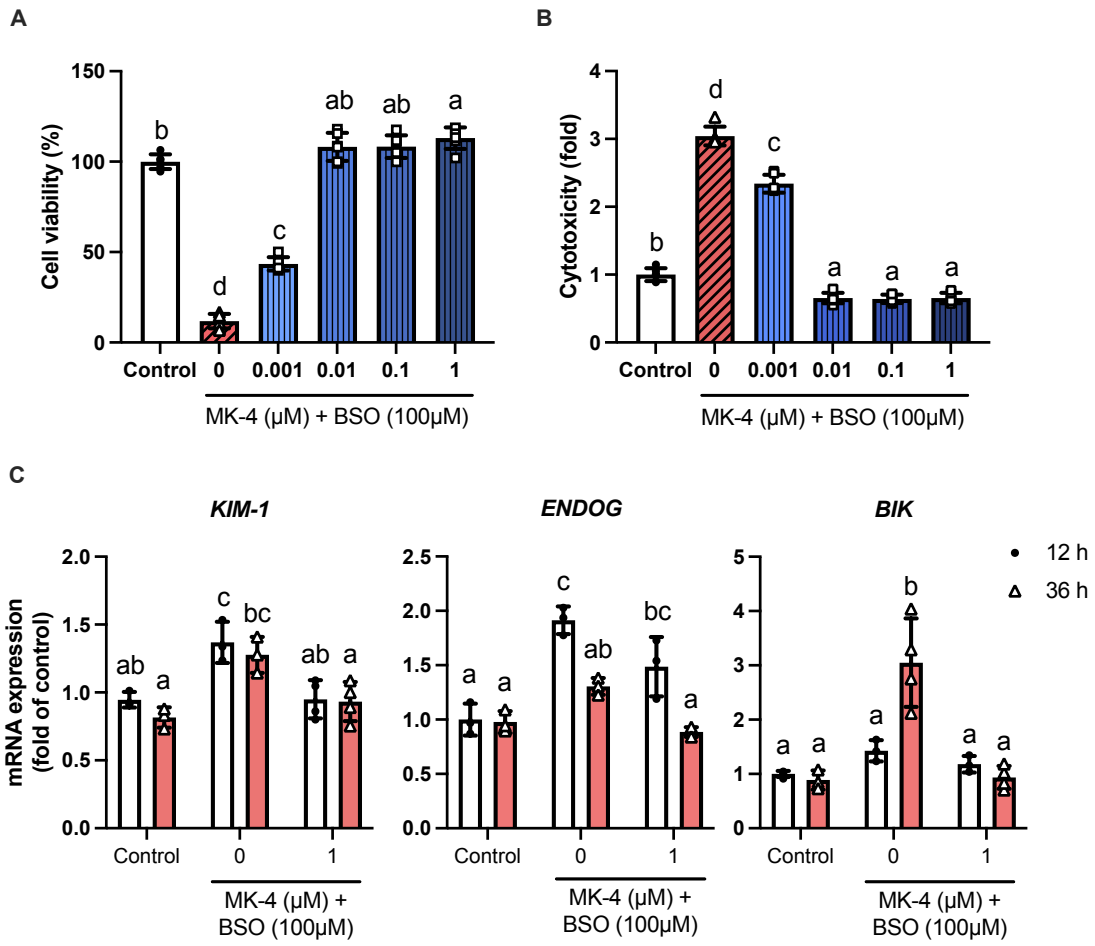
612 (A) Mitochondrial reactive oxygen species (ROS) production. Images of DHR123
613 staining to assess mitochondrial ROS levels. Scale bars = 100 μm. (B) Quantitative values
614 of DHR123 staining to assess mitochondrial ROS levels (n = 6). (C) Quantitative values
615 of mean mitochondrial length (μm) (n = 13). (D) Mitochondrial morphology. Left,
616 Images of nuclei and mitochondria using Hoechst33342 and MitoTracker green,
617 respectively. Scale bars = 50 μm. (E) Mitochondrial network features including the
618 proportion of individuals (including punctate and rods) and networks (structures with
619 branches). Values with different letters indicate significant differences at $p < 0.05$.
620
621 **Figure 4. Effect of MK-4 on mitochondrial fission in HK-2 cells treated with BSO.**
622 (A) The mRNA expression levels of fission-related genes, *DRP1* and *FIS1* (n = 3–4). (B)
623 The mRNA expression levels of fission-related genes, *DRP1* and *FIS1* (n = 3). Values
624 with different letters indicate significant differences at $p < 0.05$.
625
626 **Figure 5. Effect of MK-4 on autophagy/mitophagy in HK-2 cells treated with BSO.**

627 The mRNA expression levels of (A) autophagy-related genes, (B) ubiquitin-mediated
628 mitophagy genes, and (C) receptor-mediated mitophagy genes (n = 4). Values with
629 different letters indicate significant differences at $p < 0.05$.
630
631 **Figure 6. Effects of MK-4 on mitochondrial function in HK-2 cells treated with BSO.**
632 (A) Intracellular lactate levels (n = 3). (B) Schematic diagram of OXPHOS inhibition.
633 (C) Mitochondrial respiratory profile. Mitochondrial oxidative phosphorylation (OCR,
634 pmol/min) was measured over time using a Mito Stress Test Kit and an extracellular flux
635 analyzer. (D) The OCR parameters of OXPHOS were calculated, including basal
636 respiration, ATP-linked respiration, maximal respiration, spare respiration capacity,
637 proton-leak-linked respiration, and non-mitochondrial oxygen respiration (n = 4). Values
638 with different letters indicate significant differences at $p < 0.05$.
639
640 **Figure 7. Effects of MK-4 on mitochondrial oxygen respiration in HK-2 cells.** (A)
641 Mitochondrial respiratory profile. Mitochondrial oxidative phosphorylation was
642 measured using a Mito Stress Test Kit and an extracellular flux analyzer. (B) The OCR
643 parameters of OXPHOS were calculated, including basal respiration, ATP-linked

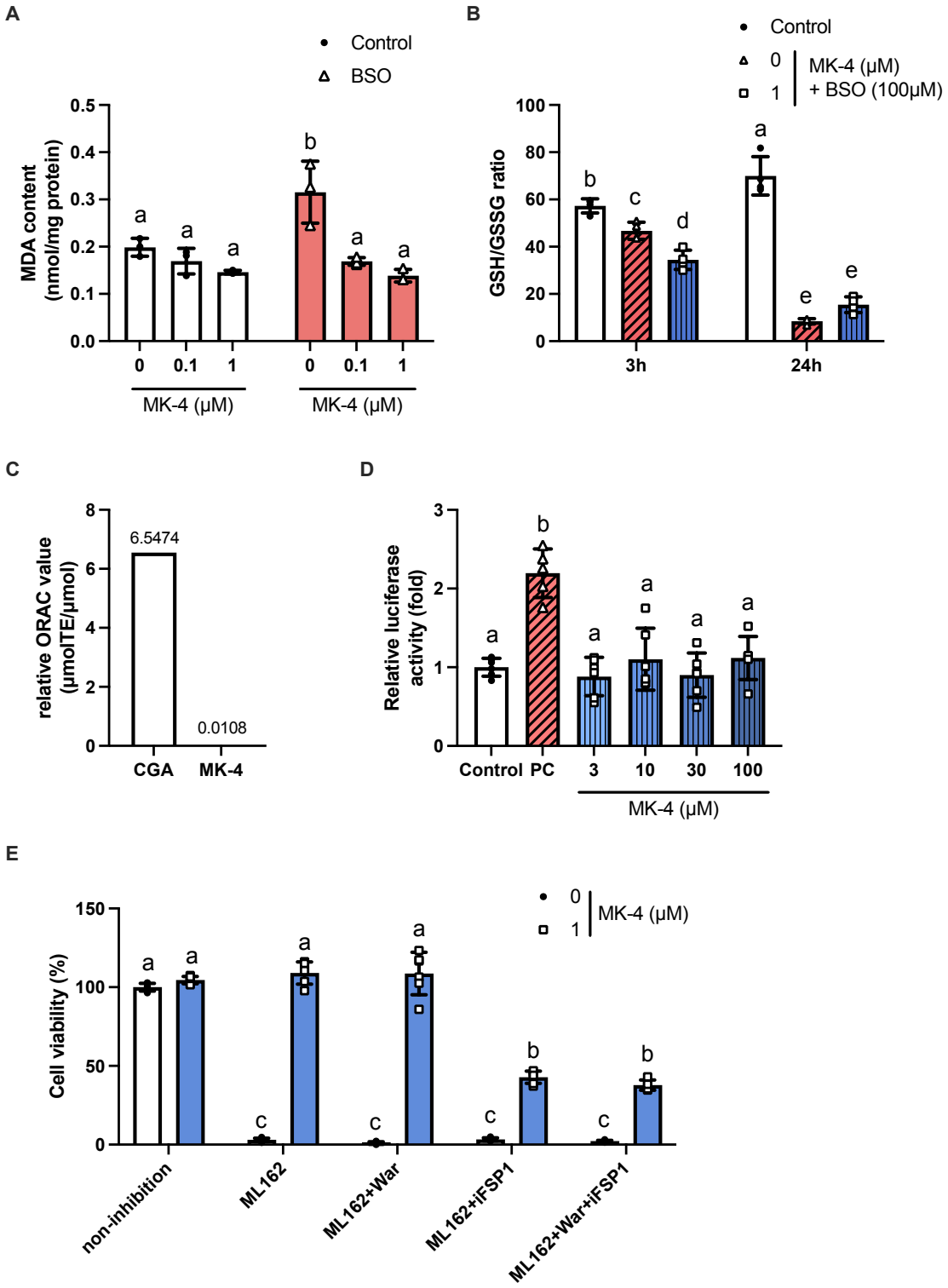
644 respiration, maximal respiration, spare respiration capacity, proton-leak-linked
645 respiration, and non-mitochondrial oxygen respiration (n = 3). (C) Intracellular ATP
646 levels (n = 6). (D) mtDNA copy number (n = 3). Values with different letters indicate
647 significant differences at $p < 0.05$.
648

Figures

Figure 1

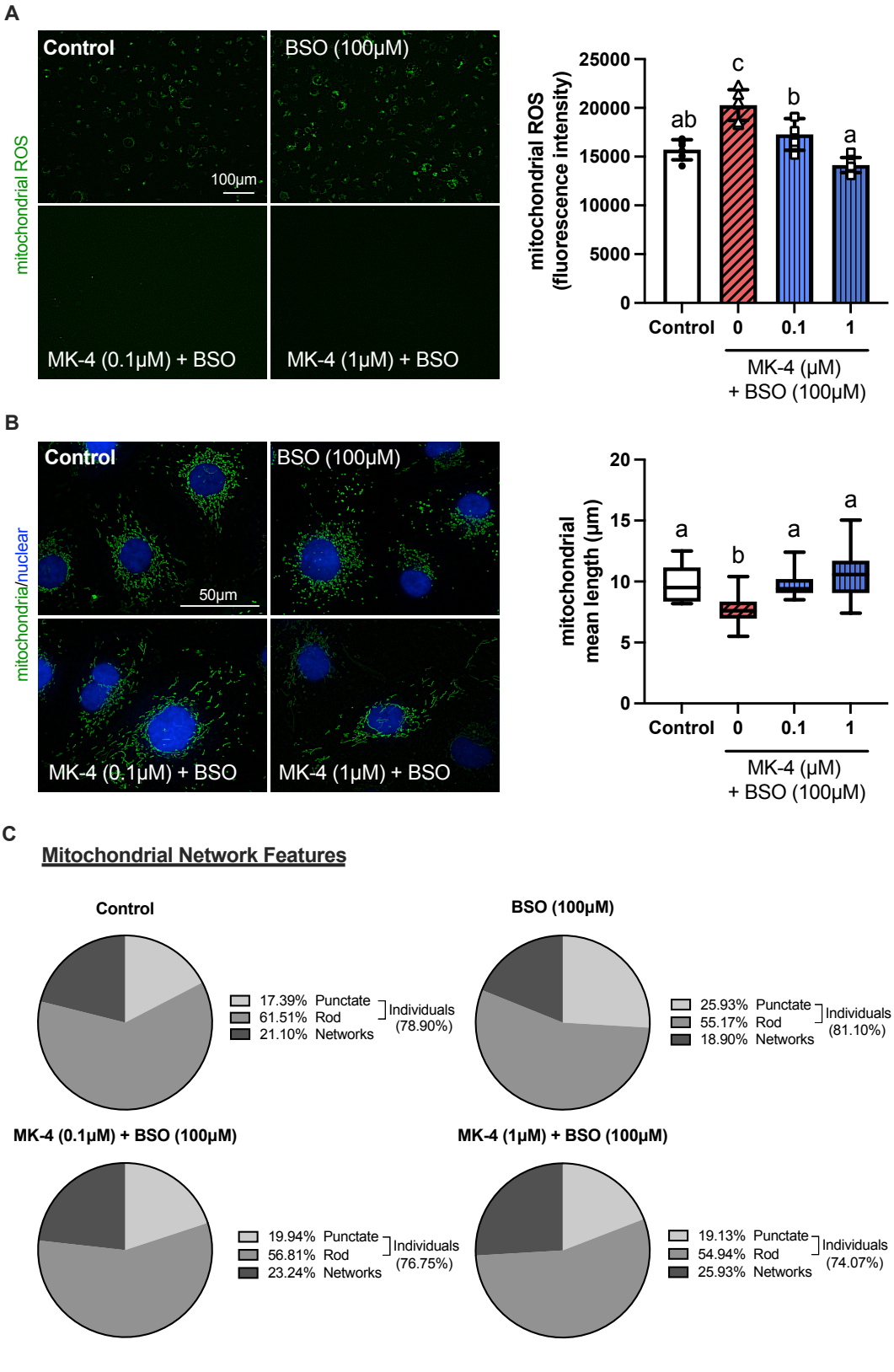


653 Figure 2



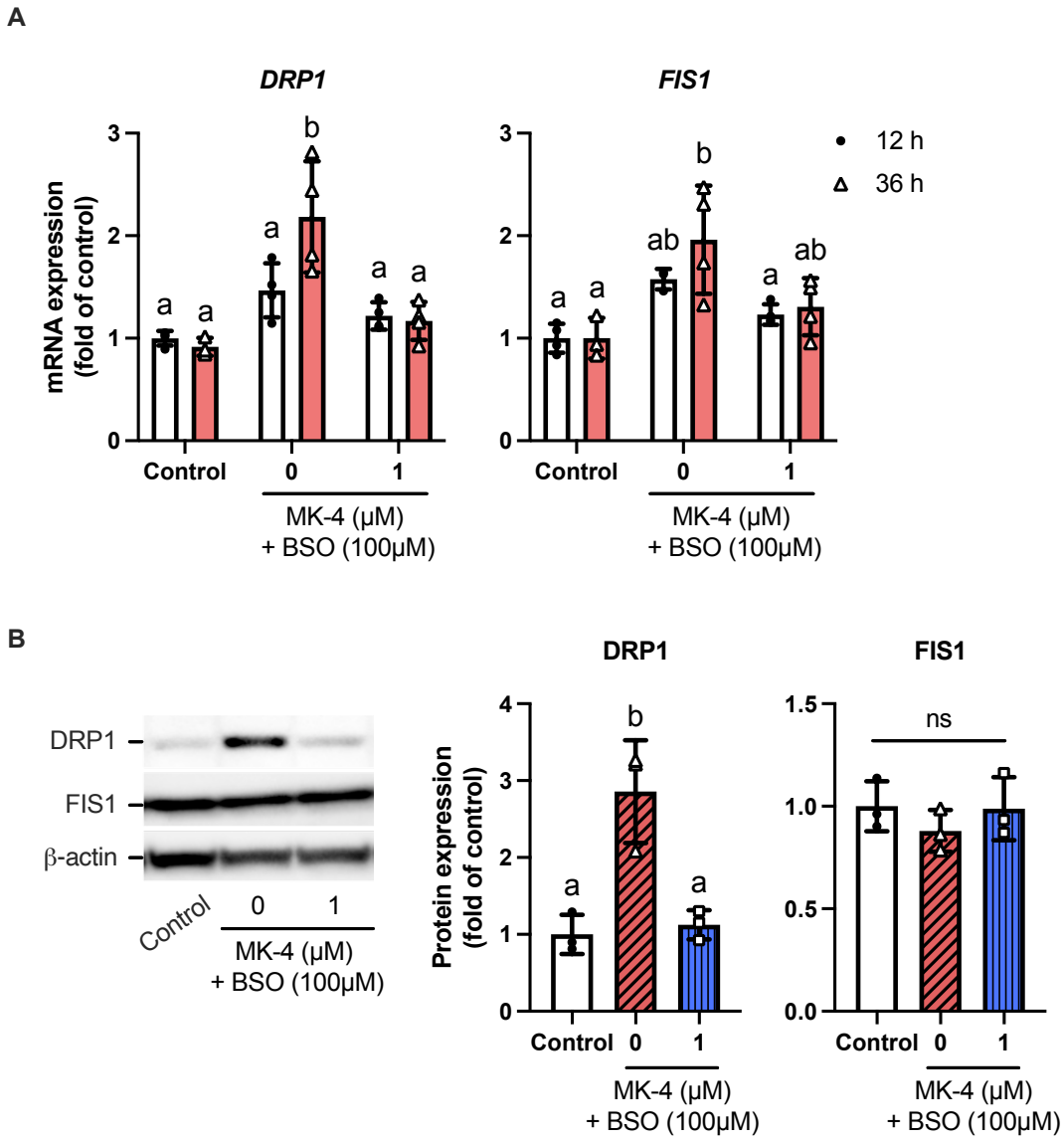
654

655 Figure 3



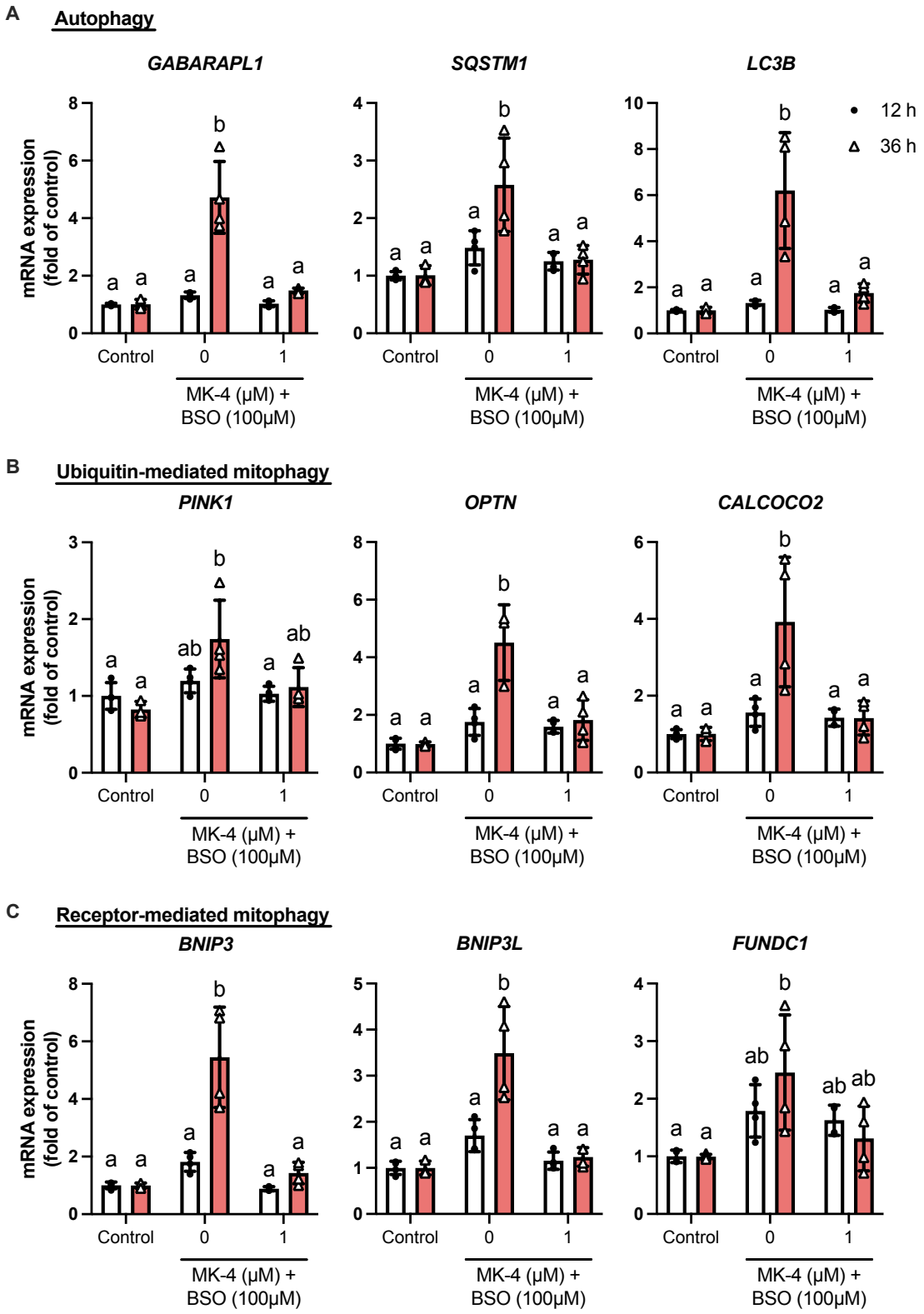
656

657 Figure 4



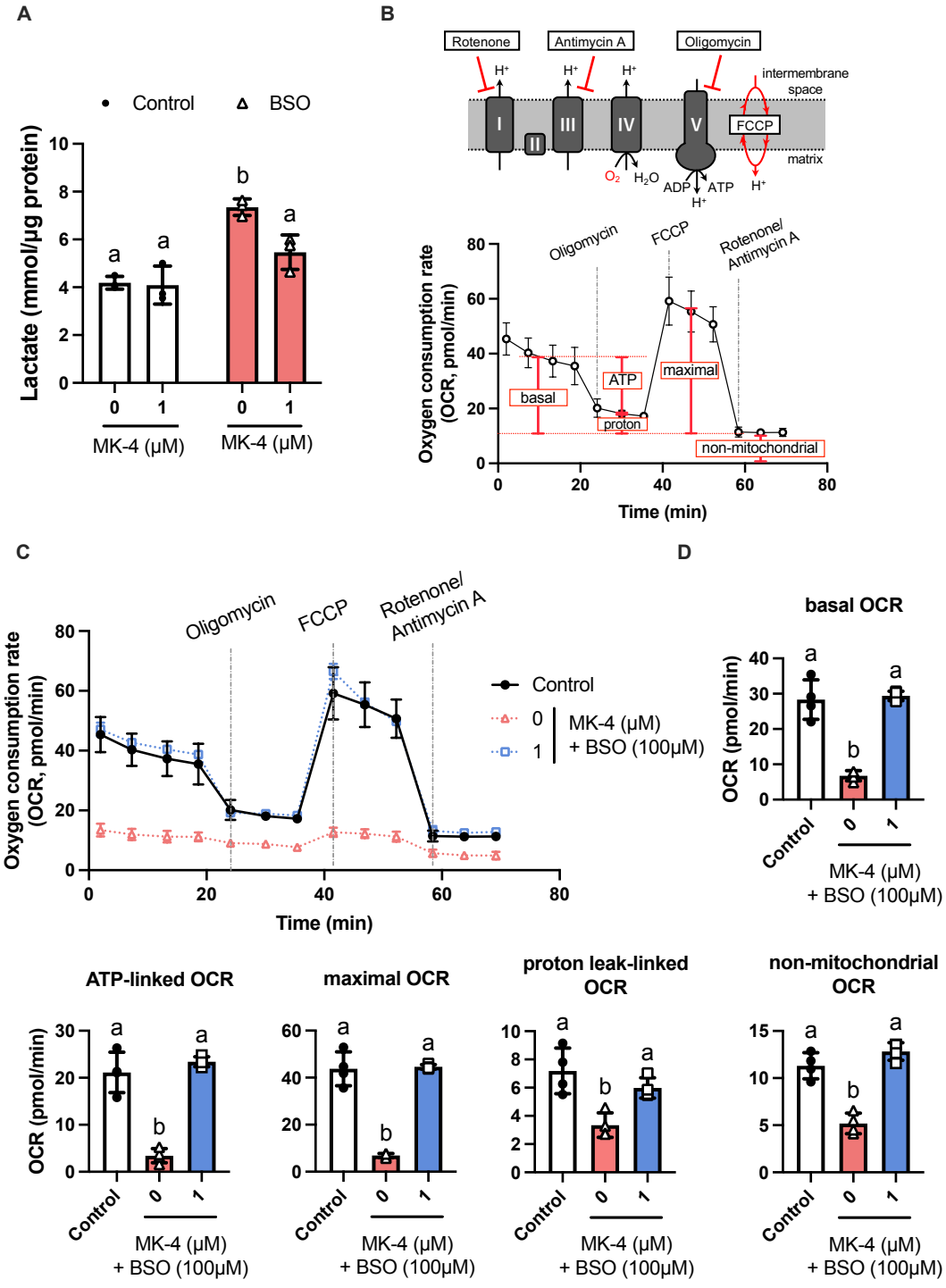
658

659 Figure 5



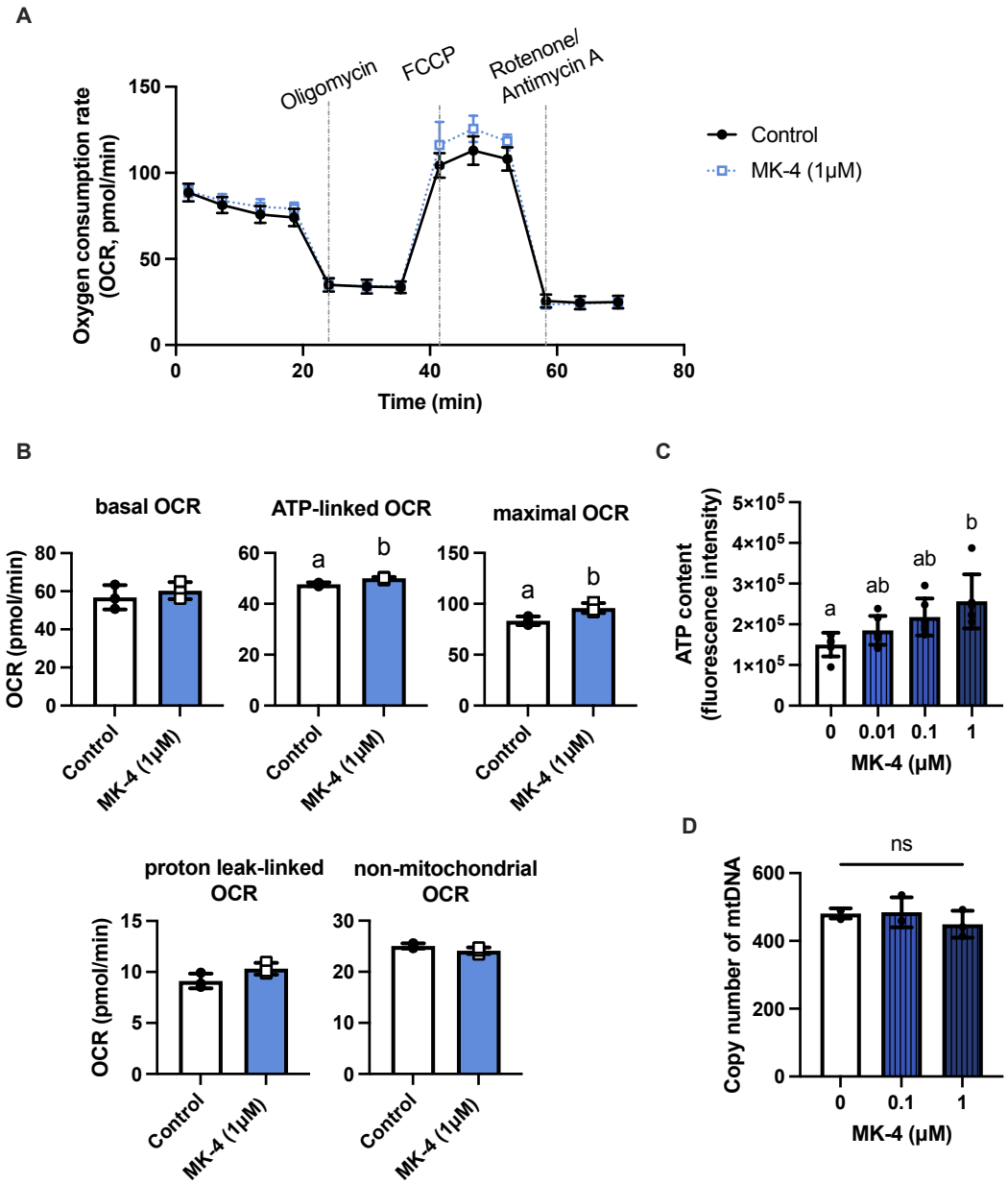
660

Figure 6


A
Control
BSO
Lactate (mmol/μg protein)
MK-4 (μM)
B
Rotenone
Antimycin A
Oligomycin
intermembrane space
matrix
FCCP
Oxygen consumption rate (OCR, pmol/min)
basal
ATP
proton
maximal
non-mitochondrial
Time (min)
C
Oligomycin
FCCP
Rotenone/ Antimycin A
Control
MK-4 (μM) + BSO (100μM)
D
basal OCR
ATP-linked OCR
maximal OCR
proton leak-linked OCR
non-mitochondrial OCR
OCR (pmol/min)

662

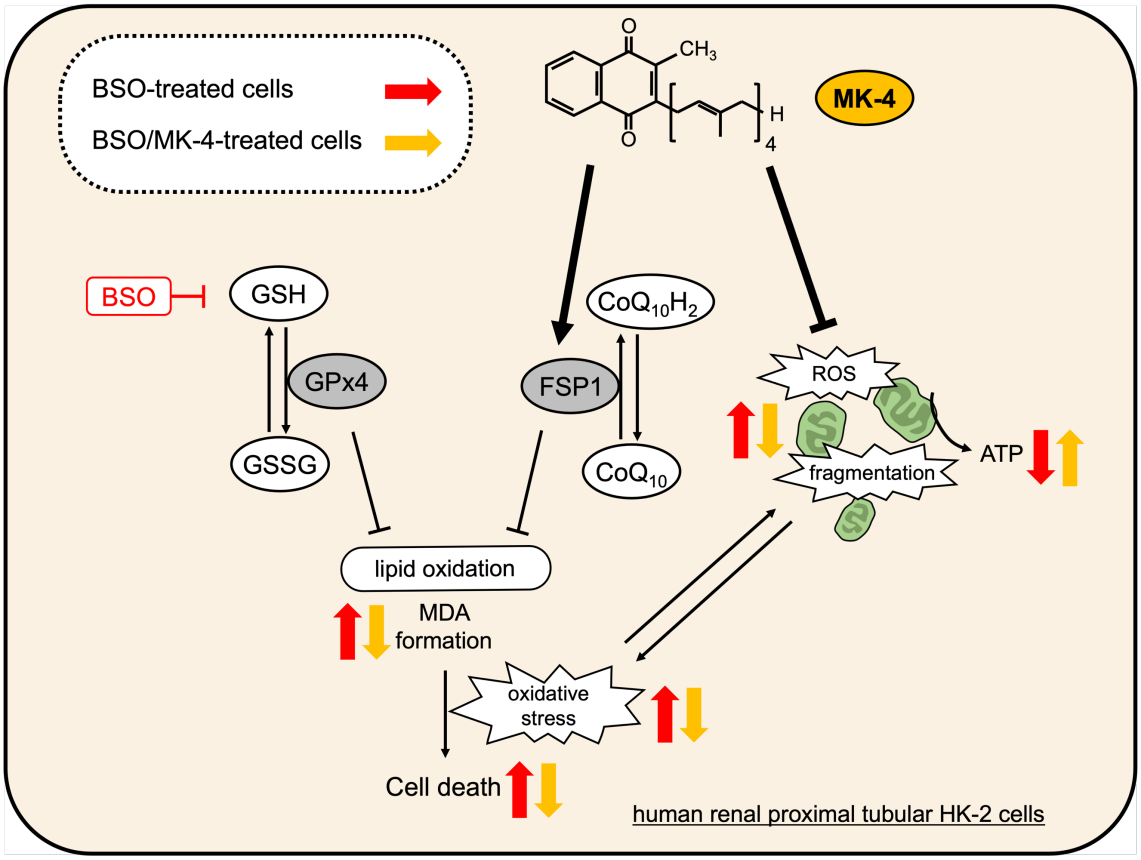
663 Figure 7



664

665

Graphic for table of contents



Caption: BSO induced oxidative stress and caused mitochondrial dysfunction, whereas MK-4 improved mitochondrial quantity by reducing mitochondrial ROS levels and regulating mitochondrial dynamics in HK-2 cells with BSO treatment.

Supporting Information: Figures S1-S2

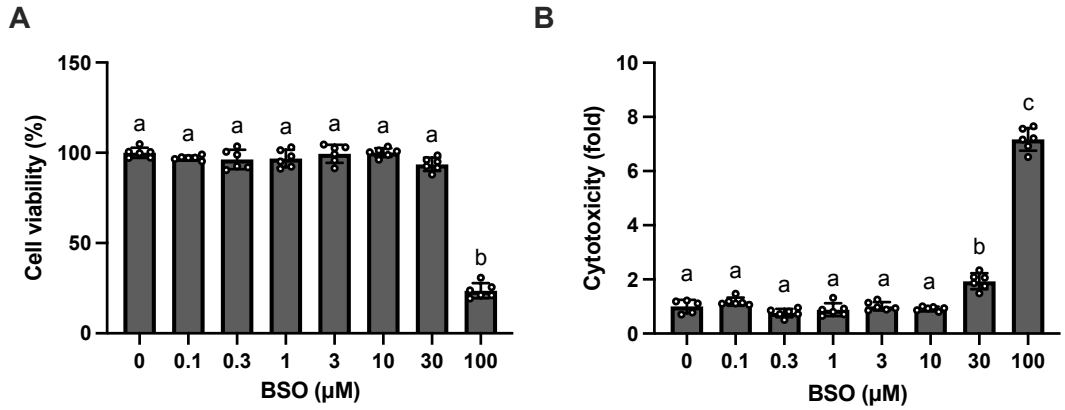


Figure S1. Cell viability and cytotoxicity were measured to assess the toxicity of BSO in HK-2 cells.

(A) The effects of BSO on cell viability (n = 6). (B) The effects of BSO on cytotoxicity (n = 5-6). BSO, L-buthionine-(S,R)-sulfoximine. Values with different letters indicate significant differences at $p < 0.05$.

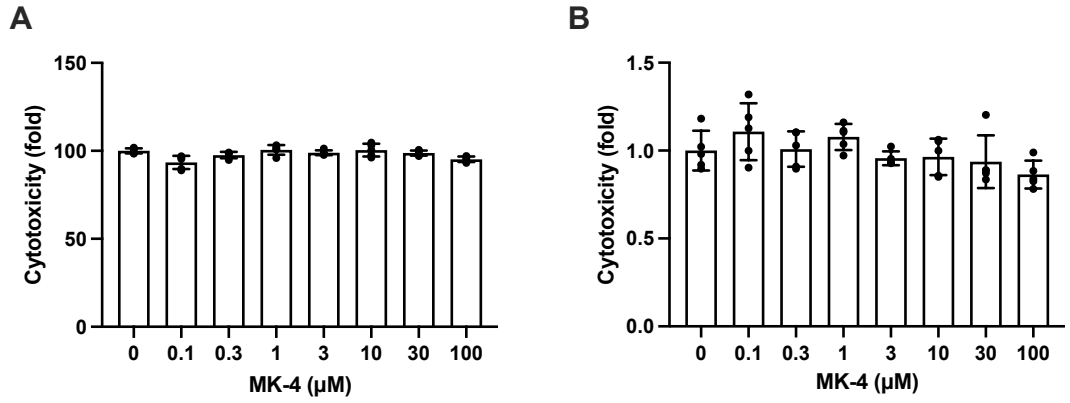


Figure S2. Cell viability and cytotoxicity were measured to assess the toxicity of MK-4 in HK-2 cells.

(A) The effects of MK-4 on cell viability (n = 5). (B) The effects of MK-4 on cytotoxicity (n = 5). MK-4, menaquinone-4.